

Paper

Int'l J. of Aeronautical & Space Sci. 15(3), 241–257 (2014)
DOI:10.5139/IJASS.2014.15.3.241

Added masses computation for unconventional airships and aerostats through geometric shape evaluation and meshing

Marco Tuveri*

Interdepartmental Centre for Industrial Research in Aeronautics, University of Bologna Italy

Alessandro Ceruti**

DIN Department, University of Bologna, Bologna, Italy

Pier Marzocca***

MAE Department, Clarkson University, Potsdam, NY, USA

Abstract

The modern development in design of airships and aerostats has led to unconventional configurations quite different from the classical ellipsoidal and spherical ones. This new class of air-vehicles presents a mass-to-volume ratio that can be considered very similar to the density of the fluid displaced by the vehicle itself, and as a consequence, modeling and simulation should consider the added masses in the equations of motion. The concept of added masses deals with the inertia added to a system, since an accelerating or decelerating body moving into a fluid displaces a volume of the neighboring fluid. The aim of this paper is to provide designers with the added masses matrix for more than twenty Lighter Than Air vehicles with unconventional shapes. Starting from a CAD model of a given shape, by applying a panel-like method, its external surface is properly meshed, using triangular elements. The methodology has been validated by comparing results obtained with data available in literature for a known benchmark shape, and the inaccuracies of predictions agree with the typical precision required in conceptual design. For each configuration, a CAD model and a related added masses matrix are provided, with the purpose of assisting the practitioner in the design and flight simulation of modern airships and scientific balloons.

Key words: Added Masses, Panel Method, Lighter Than Air Vehicles, Airships, Aerostats.

Nomenclature

\vec{a} :	vector of linear and rotational acceleration of the body	G :	added mass
a, b, c :	semi-axis of ellipsoids	h :	Green's function
C_{ij}, B_{ij} :	influence coefficients on the j -th element acting on the control point of the i -th element	L :	radius of the sphere with surface Σ considered in Green's Theorem
e :	eccentricity of the ellipsoid considered in Lamb's formula	u, v, w :	length of the airship
\vec{f}_{am} :	vector of forces and moments due to the	p, q, r :	body linear velocity along the $x, y,$ and z axis, respectively
		S_{body} :	body angular velocity around the center of buoyancy, about the $x, y,$ and z axis, respectively
			external surface of the body wetted by fluid

This is an Open Access article distributed under the terms of the Creative Commons Attribution Non-Commercial License (<http://creativecommons.org/licenses/by-nc/3.0/>) which permits unrestricted non-commercial use, distribution, and reproduction in any medium, provided the original work is properly cited.

© * Research Fellow, marco.tuveri@unibo.it
** Assistant Professor, alessandro.ceruti@unibo.it
*** Professor, Corresponding author : pmarzocc@clarkson.edu

S_{inf} :	surface of the infinite radius sphere
T :	kinetic energy of the fluid enclosed between S_{inf} and S_{body}
\ddot{u} \ddot{v} \ddot{w} \ddot{p} \ddot{q} \ddot{r} :	linear and angular acceleration, in the x, y, and z directions, and about the roll, pitch, and yaw axis, respectively
Vol :	volume of the airship
K_{am} , M_{am} , N_{am} :	AM moments around the x, y, and z axis, respectively
X_{am} , Y_{am} , Z_{am} :	AM forces along the x, y, and z axis, respectively
α , β , γ :	normal cosines direction of the boundary elements (QUAD, TRIA) of the surface, respectively
δ , ϑ :	parameters used to compute explicit value of elongated ellipsoid with Lamb's formula
Φ :	flow potential
Φ_l :	potential on the lower side of a trailing edge of a streamlined body
Φ_u :	potential on the upper side of a trailing edge of a streamlined body
Φ_w :	potential on the wake surface leaving the trailing edge of a streamlined body
λ_{ik} :	added masses coefficients
ρ :	density of the fluid surrounding the body

Acronyms

AM:	added masses
CB:	center of buoyancy
DOF:	degrees of freedom
BEM:	Boundary Element Method

1. Introduction

In recent years, there has been a renewed interest in airships and aerostats, due to the advancement of new technologies and materials, and the increasing need for environmentally friendly and sustainable ways of transport. The availability of thin photovoltaic arrays capable of converting the energy provided by solar radiation into electricity, and the development of new thin fabrics with very good strength-to-weight ratio and low permeability to gases have enabled successful feasibility studies of high altitude solar airships. In solar powered airships, the power available to the propulsion plant depends on the efficiency of the solar film, and on the shape of the airship. The amount of surface covered by solar film, and its orientation with respect to the incident solar rays, play

a fundamental role in solar energy capture. On the other hand, the geometry of the airship strongly affects the volume-to-surface ratio and the aerodynamic drag; the first is important, since the buoyancy is mainly affected by the volume (and the airship weight is proportional to the envelope surface); while the drag is strongly linked to the power needed to guarantee a defined speed. The classical ellipsoidal shape, universally described as the best solution from the early era of airships, up to the end of the past millennium [1], guarantees a very good volume-to-weight ratio and a low drag; however, this configuration has very low surface available for solar panels, which limits its applicability to energetically sustainable airships. Due to this limit, while dealing with solar configurations, a plethora of innovative configurations has recently been proposed, which configurations are in many respects unconventional. Several of these have been evaluated [2], in order to obtain large top surfaces, low drag, and good volume-to-weight ratio. A new method for airship design and weight evaluation was proposed by Ref. [3], while Ref. [4] provided a state-of-the-art review for the design and analysis of this new class of airships. The current literature does not adequately address the importance of the added masses, and these studies indicated that the classical formulae used for added masses computation introduced for ellipsoidal shapes are not valid for the unconventional airship configurations. The problem of added masses for a new configuration was introduced by Ref. [5], albeit for a specific shape of hybrid airship; while Ref. [2] suggested the computation of an equivalent ellipsoid shape, which approximates the actual unconventional shape.

To supplement the state-of-the-art understanding in this important but often overlooked aspect, this paper provides added masses data for a number of new airship configurations that are collected and computed herein; this data can be useful for developing flight simulators and dynamic models, for studying the behavior of airships, and for advancing their control systems strategies. Data about scientific balloons are also presented: in this case the shape of the envelope changes, during the climb to the design altitude. These balloons are usually partially inflated on the ground [6], while during climbing, the inside gas can expand, without significantly increasing the pressure acting on the envelope. While on the ground, the lifting gas fills only the upper part of the balloon; hence, the balloon does not assume the typical spherical shape, but a more streamlined one. If good precision is required in the study of the balloon's ascent phase, the added masses contributions of the balloon actual shape (which depends on the internal pressure of the lifting gas and altitude) should be carefully evaluated.

The added masses concept is related to the fact that an accelerated body affects the fluid field in which it is immersed, and consequently increases the kinetic energy

in the fluid. The term “added masses” is usually defined as the inertia of the mass of fluid displaced by the body. The added masses term should always be included in the motion equation; but when the mass of the fluid displaced is smaller than the mass of the vehicle itself (this is usually the case for aircraft), the term is often neglected. For instance, Ref. [2] computes the ratio between the air mass displaced by a Boeing 747 and its mass equal to 0.01, while this value jumps to 770 for an air bubble moving into water. Added masses provide critical effects in the motion equations of vehicles like airships, balloons, submarine vehicles, and ships, and should be considered by their designers. According to the work by Ref. [7], the concept of added mass was introduced by Dubua in 1776, following the experiment study of the small oscillations of a spherical pendulum proposed by Ref. [8]; afterwards, Green in 1833 and Stokes in 1843 [9] focused their attention on the sphere, computing an exact mathematical expression of the added masses. At the beginning of the past century, several studies were carried out to compute added masses for bodies with two or three planes of symmetry: in particular the interest focused on airships whose shape was axial-symmetric. One of the seminal works related to added masses was published by Lamb in 1918 [10]; it presents added masses coefficients for ellipsoid-based shapes, and it is still used for the computation of added masses for traditional shaped airships. Munk [11] in 1924 presented a similar study to compute the added masses coefficient, later used by airship designers to take this effect into account. In succession, Implay [12] in 1961 considered the problem of added masses, with the study of the expression for added mass of a rigid body moving in an ideal fluid. With the introduction of computers and algorithms, the panel method developed in aerodynamics was applied to compute the added mass coefficients matrix; in this way, the solution of potential equations on complex geometries was possible, by exploiting the computing capabilities of machines. These methodologies, originated in the early 1960’s, are still attractive, because the governing equations need to be solved at the boundary [7], and the current computing capabilities are adequate, and continually improving. An implementation of the panel method by the authors (discussed in the later section), allows arbitrary shapes to be considered. Furthermore, the method provides advantages over a volume mesh typical of Finite Difference, Finite Volume, or Finite Element methods, assuring the efficient solution of a lower dimensional system of equations. Birkhoff [8] generalized the added mass computation mathematical framework to an arbitrary body moving in different (laminar and turbulent) flow regimes. However, explicit closed-loop formulae for computing added masses are only available for simple bodies. The Laplace equation with boundary conditions given on the surface of the body

and at infinity should be solved, to compute the added masses. The most widespread solution methods are based on the separation of variables, and the singularity method developed and introduced by Refs. [13], [14], and [15]. Following Ref. [16], an explicit solution is now available, albeit only for the oblate spheroid, elongated ellipsoid of revolution, sphere, disc, and elliptic plates. In marine applications, the problem of added masses is addressed for slender bodies like ships, in which one dimension is usually greater than the other two (e.g. a cylinder); in this case, as discussed by Ref. [9], the added mass coefficient matrix could be computed with the plane section method in orthogonal directions, with respect to the axis along the largest dimension. The same author proposes exploiting the method of an equivalent ellipsoid in complex cases, computing the approximated added mass coefficients, considering a body with the same volume of a three axial ellipsoid. A similar concept was presented in Ref. [2], but the estimation is inaccurate for the complex and irregular shapes typical of modern unconventional airships, although it can be considered a way to provide preliminary added masses estimates. Another approach to added masses computation is by performing experimental tests; this has been applied, for instance, to swimmers [17]. Other authors like Refs. [18] and [19] developed frameworks to compute added masses for airships whose shape can be approximated with mathematical expressions. However, due to the recent interest in unconventional airship configurations, and the huge number of developed unconventional configurations, their designers should be provided with better estimates of added masses, thus enabling precise simulations of airship dynamics, which is quite important in the case of complex shapes.

This paper presents a methodology to compute the full matrix of added masses for bodies of arbitrary shape, exploiting a method based on the Boundary Element Method; it presents also some examples of unconventional airship shapes, and provides data about their added masses contributions. Moreover, the proposed method allows finding the best trade-off between computational time and results accuracy, by defining the mesh size. The rest of the paper is organized as follows: the next section provides the mathematical framework lying behind the computation of added masses and their modern implementation on computers. The third section presents considerations about method validation and benchmarks with literature, the influence of the mesh definition on the obtained results, and the needs for meshing the external geometry of bodies, along with the definition and computation of the dimensionless coefficients. The fourth section provides added masses tables for 20 airship and balloon shapes. The paper concludes with pertinent remarks.

2. Mathematical framework and implementation

2.1 Added masses matrix features

The response of a body to an applied force in a specific direction generally induces an acceleration that involves three translation and three angular accelerations [20]:

$$\vec{a} = \{\dot{u} \quad \dot{v} \quad \dot{w} \quad \dot{p} \quad \dot{q} \quad \dot{r}\}^T \quad (1)$$

The six force components generated from the added masses effect, identified with subscript “am”, are

$$\vec{f}_{am} = \{X_{am} \quad Y_{am} \quad Z_{am} \quad K_{am} \quad M_{am} \quad N_{am}\}^T \quad (2)$$

As a result, the inertial effects of the fluid, due to the six possible components of acceleration imposed on the body, can be identified by

$$\vec{f}_{am} = -M_a \vec{a} \quad (3)$$

where, the added mass matrix M_a for a body, considering the six DOF, is expressed as:

$$-M_a = \begin{bmatrix} X_{\dot{u}} & X_{\dot{v}} & X_{\dot{w}} & X_{\dot{p}} & X_{\dot{q}} & X_{\dot{r}} \\ Y_{\dot{u}} & Y_{\dot{v}} & Y_{\dot{w}} & Y_{\dot{p}} & Y_{\dot{q}} & Y_{\dot{r}} \\ Z_{\dot{u}} & Z_{\dot{v}} & Z_{\dot{w}} & Z_{\dot{p}} & Z_{\dot{q}} & Z_{\dot{r}} \\ K_{\dot{u}} & K_{\dot{v}} & K_{\dot{w}} & K_{\dot{p}} & K_{\dot{q}} & K_{\dot{r}} \\ M_{\dot{u}} & M_{\dot{v}} & M_{\dot{w}} & M_{\dot{p}} & M_{\dot{q}} & M_{\dot{r}} \\ N_{\dot{u}} & N_{\dot{v}} & N_{\dot{w}} & N_{\dot{p}} & N_{\dot{q}} & N_{\dot{r}} \end{bmatrix} \quad (4)$$

Computing all coefficients of this matrix, and identifying the negligible one, is a task that can be quite challenging. If an external additional force is applied to the body, acceleration arises in all six components; simplifications to compute the matrix coefficients can be made, by considering the flow surrounding the body as potential. As a consequence of the potential flow assumption, it can be shown that the added masses matrix must be symmetric, and hence the number of coefficients in the matrix is reduced from 36 to 21.

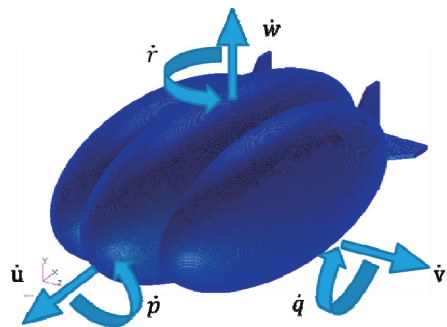


Fig.1. axis reference system

$$-M_a = \begin{bmatrix} X_{\dot{u}} & X_{\dot{v}} & X_{\dot{w}} & X_{\dot{p}} & X_{\dot{q}} & X_{\dot{r}} \\ & Y_{\dot{v}} & Y_{\dot{w}} & Y_{\dot{p}} & Y_{\dot{q}} & Y_{\dot{r}} \\ & & Z_{\dot{w}} & Z_{\dot{p}} & Z_{\dot{q}} & Z_{\dot{r}} \\ & & & K_{\dot{p}} & K_{\dot{q}} & K_{\dot{r}} \\ & & & & M_{\dot{q}} & M_{\dot{r}} \\ sym & & & & & N_{\dot{r}} \end{bmatrix} \quad (5)$$

Additional reductions are possible for submerged bodies that own particular symmetry properties, as explained next. For bodies with one single plane of symmetry (e.g. plane of symmetry $z=0$), any acceleration limited to this plane, specifically $(\dot{u}, \dot{v}, \dot{r})$, will produce no added mass forces, defined as (Z_{am}, K_{am}, M_{am}) ; the only possible non-zero forces will be (X_{am}, Y_{am}, N_{am}) . Consequently, the added masses matrix will include only 12 non-zero constants:

$$-M_a = \begin{bmatrix} X_{\dot{u}} & X_{\dot{v}} & 0 & 0 & 0 & X_{\dot{r}} \\ & Y_{\dot{v}} & 0 & 0 & 0 & Y_{\dot{r}} \\ & & Z_{\dot{w}} & Z_{\dot{p}} & Z_{\dot{q}} & 0 \\ & & & K_{\dot{p}} & K_{\dot{q}} & 0 \\ & & & & M_{\dot{q}} & 0 \\ sym & & & & & N_{\dot{r}} \end{bmatrix} \quad (6)$$

If a body has two planes of symmetry, the number of non-zero constants in the AM matrix further reduces. As an example, if the symmetry planes are $y=0$ and $z=0$, the resulting AM matrix is:

$$-M_a = \begin{bmatrix} X_{\dot{u}} & 0 & 0 & 0 & 0 & 0 \\ & Y_{\dot{v}} & 0 & 0 & 0 & Y_{\dot{r}} \\ & & Z_{\dot{w}} & 0 & Z_{\dot{q}} & 0 \\ & & & K_{\dot{p}} & 0 & 0 \\ & & & & M_{\dot{q}} & 0 \\ sym & & & & & N_{\dot{r}} \end{bmatrix} \quad (7)$$

The moment about the z axis generated by acceleration in the y direction, and the moment about the y axis generated by acceleration in the z direction, can be represented by the remaining off-diagonal terms. In other words, since the body is not symmetric about the $z = 0$ plane, pitching moments in the xy or xz planes will be caused by linear acceleration in either the y or z direction. In the case of three axes of symmetry, the matrix becomes purely diagonal, since there are no secondary induced accelerations.

2.2 Dimensionless AM coefficients

Following the approach introduced in [21], the added mass coefficients for a body moving in a fluid are expressed in dimensionless form, where the length of the vehicle appears with different power. Specifically, the following rules are adopted:

1. The coefficients representing the effect of a force on a linear acceleration use ρl^3 . The cube of the

length represents the volume of the vehicle, which is proportional to the mass of water displaced by the outer hull.

2. The coefficients representing the effect of time on an angular acceleration use ρl^5 .
3. The remaining coefficients, representing the effects of a force on an angular acceleration, or the effect of a moment on a linear acceleration, use ρl^4 .

This implies that for a body moving in a potential flow, the AM coefficients matrix in non-dimensional form can be expressed as:

$$-\overline{M}_a = \begin{bmatrix} \frac{X_{\dot{u}}}{\rho l^3} & \frac{X_{\dot{v}}}{\rho l^3} & \frac{X_{\dot{w}}}{\rho l^3} & \frac{X_p}{\rho l^4} & \frac{X_q}{\rho l^4} & \frac{X_r}{\rho l^4} \\ & \frac{Y_{\dot{v}}}{\rho l^3} & \frac{Y_{\dot{w}}}{\rho l^3} & \frac{Y_p}{\rho l^4} & \frac{Y_q}{\rho l^4} & \frac{Y_r}{\rho l^4} \\ & & \frac{Z_{\dot{w}}}{\rho l^3} & \frac{Z_p}{\rho l^4} & \frac{Z_q}{\rho l^4} & \frac{Z_r}{\rho l^4} \\ & & & \frac{K_p}{\rho l^5} & \frac{K_q}{\rho l^5} & \frac{K_r}{\rho l^5} \\ & & & & \frac{M_q}{\rho l^5} & \frac{M_r}{\rho l^5} \\ & & & & & \frac{N_r}{\rho l^5} \end{bmatrix} \quad (8)$$

sym

2.3 Mathematical framework

The definition of a scalar potential field is fundamental to the computation of added masses. The assumption is that a body moving with a constant acceleration in an incompressible potential flow can be represented by a scalar potential field Φ . The fluid velocity at point \vec{r} with respect to the origin can be expressed as:

$$\vec{U}(\vec{r}, t) = \nabla \phi(\vec{r}, t) \quad (9)$$

For an incompressible fluid, the continuity equation is:

$$\nabla \cdot \vec{U} = 0 \quad (10)$$

and substituting Eq. (8) in Eq. (9) one obtains the Laplace's equation, which is valid for inviscid, incompressible, and irrotational flow.

$$\nabla^2 \phi = 0 \quad (11)$$

The boundary conditions necessary for the solution of the Laplace's equation are as follows:

1. The watertight condition, valid on the surface S

$$\frac{\partial \phi}{\partial \hat{n}} \Big|_S = u_n \quad (12)$$

where, \hat{n} is the external normal direction to surface S, while u_n is the projection of velocity of a point of the body on the normal \hat{n} .

2. Stationary condition at infinity:

$$\lim_{r \rightarrow \infty} \frac{\partial \phi}{\partial r} = 0 \quad (13)$$

where, r is the distance from the origin to the fluid point.

3. Inviscid lifting flows invoke the Kutta condition to enforce pressure continuity, in order to ensure that the flow at the trailing edge leaves smoothly. Wake sheet potential must equal the potential jump of the upper and lower part of the trailing edge, so as to keep pressure continuity [22], see Fig. 2.

Since non-lifting flow is considered here, there was no need to apply the Kutta condition, which for the sake of completeness is reported as $\phi_u - \phi_l = \phi_w$.

The condition (11) has to be examined in more detail. Assuming $\vec{u}_0(u_{0x}, u_{0y}, u_{0z})$ to be the velocity of a point 0 of the body, and $\vec{\omega}(\omega_x, \omega_y, \omega_z)$ as the angular velocity of the body with respect to the point 0, the velocity of an arbitrary point of the body, including any point on its surface S, is straightforwardly determined by the relation:

$$\vec{u} = \vec{u}_0 + \vec{\omega} \times \vec{r} \quad (14)$$

where, \vec{r} is the vector that indicates the position of the point.

This vector equation can be written in basic components, such as:

$$\begin{aligned} u_x &= u_{0x} + \omega_y z - \omega_z y \\ u_y &= u_{0y} + \omega_z x - \omega_x z \\ u_z &= u_{0z} + \omega_x y - \omega_y x \end{aligned} \quad (15)$$

The projection of velocity on the normal \hat{n} on the surface S is:

$$u_n = u_x \cos(n, x) + u_y \cos(n, y) + u_z \cos(n, z) \quad (16)$$

For the sake of simplicity, the following abbreviations are chosen:

$$\alpha = \cos(n, x); \quad \beta = \cos(n, y); \quad \gamma = \cos(n, z) \quad (17)$$

in order to write the watertight condition as:

$$\begin{aligned} \frac{\partial \phi}{\partial \hat{n}} \Big|_S &= u_n = u_{0x} \alpha + u_{0y} \beta + u_{0z} \gamma + \omega_x (\gamma y - \beta z) \\ &+ \omega_y (\alpha z - \gamma x) + \omega_z (\beta x - \alpha y) \end{aligned} \quad (18)$$

where, $\alpha, \beta, \gamma, (\gamma y - \beta z), (\alpha z - \gamma x), (\beta x - \alpha y)$ depend only on the body's shape. Assuming linearity, the fluid potential

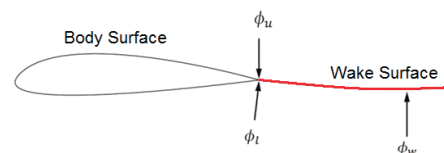


Fig. 2. Body moving in the domain with wake surface

can be written as follows:

$$\phi = u_{0x}\phi_1 + u_{0y}\phi_2 + u_{0z}\phi_3 + \omega_x\phi_4 + \omega_y\phi_5 + \omega_z\phi_6 \quad (19)$$

The potentials ϕ_i are such that $i=1,2,3$ are for the body moving along the x,y,z axes, while $i=4,5,6$ are for the body rotating around the same axes with unit angular velocities. The solution of the Laplace problem can be found by subdividing it into 6 sub-problems. The first one can be formulated for the solution of the Laplace equation $\nabla^2\phi_1 = 0$, with the watertight condition on the surface S :

$$\frac{\partial\phi}{\partial\hat{n}}\Big|_S = \alpha \quad \text{and} \quad \lim_{r\rightarrow\infty} \frac{\partial\phi_1}{\partial r} = 0 \quad (20, 21)$$

It is very important to note that all the potentials are only functions of the body's shape, and of the choice of the coordinate system attached to the body. The added masses computation follows the evaluation of the kinetic energy of the displaced fluid: assume a body with surface S , moving in a fluid bounded by a sphere with surface Σ and radius h , containing the body. The kinetic energy of the fluid displaced by the body can be defined by the integral:

$$T = \frac{1}{2}\rho \int_V v^2 dV = \int_V \left[\left(\frac{\partial\phi}{\partial x}\right)^2 + \left(\frac{\partial\phi}{\partial y}\right)^2 + \left(\frac{\partial\phi}{\partial z}\right)^2 \right] dx dy dz \quad (22)$$

here, ρ is the density of the fluid. Using Green's transformation for two function (ϕ_a, ϕ_b) , one obtains:

$$\int_V \nabla\phi_a \nabla\phi_b dV = - \int_{S+\Sigma} \phi_a \frac{\partial\phi_b}{\partial\hat{n}} dS - \int_V \phi_a \nabla^2\phi_b dV \quad (23)$$

By considering $\phi_a = \phi_b = \phi$, and recalling the initial condition $\nabla^2\phi = 0$, the kinetic energy can be cast as:

$$T = -\frac{\rho}{2} \int_S \phi \frac{\partial\phi}{\partial\hat{n}} dS - \frac{\rho}{2} \int_\Sigma \phi \frac{\partial\phi}{\partial\hat{n}} dS \quad (24)$$

It is straightforward to note that the two integrals are identical, but for the surfaces on which they are applied. The second integral can be considered negligible, due to the asymptotical behavior of ϕ as $h\rightarrow\infty$ (where h is the radius of the sphere with surface Σ), and of its first derivative as $|\vec{r}|\rightarrow\infty$. As a result:

$$T = -\frac{\rho}{2} \int_S \phi \frac{\partial\phi}{\partial\hat{n}} dS \quad (25)$$

By substituting Eq. (19) into Eq. (25), and writing:

$$\begin{aligned} u_{0x} &= u_1; & u_{0y} &= u_2; & u_{0z} &= u_3 \\ \omega_x &= u_4; & \omega_y &= u_5; & \omega_z &= u_6 \end{aligned} \quad (26)$$

the kinetic energy can be further simplified, to read:

$$T = \frac{1}{2} \sum_{i,k=1}^6 \lambda_{ik} u_i u_k \quad (27)$$

where, λ_{ij} are the added masses, and can be expressed as:

$$\lambda_{ik} = -\rho \int_S \frac{\partial\phi_i}{\partial\hat{n}} \phi_k dS \quad (28)$$

Observing the last equation, it can be noted that λ_{ik} does not depend on the kinematic of the motion, but only on the body's shape. By applying Green's formula to the functions ϕ_i and ϕ_k on the volume V between the surface S and Σ , one obtains:

$$\begin{aligned} \int_V (\phi_i \Delta\phi_k - \phi_k \Delta\phi_i) dV &= \int_S \left(\phi_i \frac{\partial\phi_k}{\partial\hat{n}} - \phi_k \frac{\partial\phi_i}{\partial\hat{n}} \right) dS \\ &- \int_\Sigma \left(\phi_i \frac{\partial\phi_k}{\partial\hat{n}} - \phi_k \frac{\partial\phi_i}{\partial\hat{n}} \right) dS \end{aligned} \quad (29)$$

Equation (11) leads to $\Delta\phi_k = \Delta\phi_i = 0$; hence, the left-hand side of the equation is negligible, while the second integral of the right-hand side is negligible as $h\rightarrow\infty$ [9] (where h is the radius of the sphere with surface Σ). Therefore, the infinite fluid surrounding the body withstands the following condition:

$$\int_S \phi_i \frac{\partial\phi_k}{\partial\hat{n}} dS = \int_S \phi_k \frac{\partial\phi_i}{\partial\hat{n}} dS \quad (30)$$

Consequently, it can be stated that $\lambda_{ik} = \lambda_{ki}$. As indicated earlier, the number of constants to be determined is reduced from 36 to 21, due to the symmetry of the added mass matrix.

The final step to consider is the boundary integral equation evaluation. Consider a closed region V with boundary S and the unit vector \hat{n} normal to S , as depicted in Fig. 3. Boundary S of the flow region includes the surface of the body S_b , the surface of the wake SW , and the outer control surface S_∞ . The latter includes the surface of the body and the trailing vortex surface.

Using Green's theorem, the perturbation velocity potential at each point of the field can be expressed as an integral equation corresponding to the distribution of the source and the dipole. Therefore, for the field point P in the region V , this is [23]:

$$\begin{aligned} 2\pi\phi(P) &= \int_{S_B} \phi(Q) \frac{\partial G}{\partial\hat{n}} dS - \int_{S_B} \frac{\partial\phi(Q)}{\partial\hat{n}} G dS + \\ &+ \int_{S_w} \Delta\phi(Q) \frac{\partial G}{\partial\hat{n}} dS \end{aligned} \quad (31)$$

where, G is the Green's function, which might be expressed in the form $G=1/r$, and r is the distance between the point

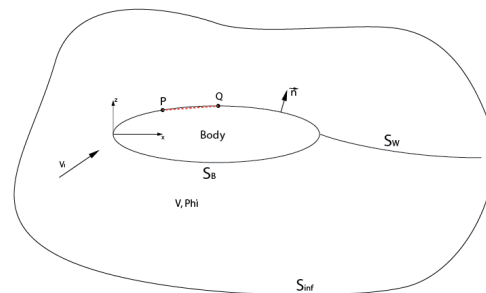


Fig. 3. Green's theorem on the body

field P and point source Q . The boundary conditions to be applied are reported in the previous section. The right-hand side of Eq. (31) has three terms. The first two are the dipole and the source of the body, while the third is the dipole of the vortex wake surface (defined only for lifting bodies).

2.4 Numerical Implementation

The discretization of Eq. (31) leads to a linear system of algebraic equations for the unknown ϕ as:

$$2\pi\phi_i(P) = \sum_{j=1}^{N_B} \phi_j(Q_i) C_{ij} - \sum_{j=1}^{N_B} \frac{\partial\phi}{\partial n}(Q_i) B_{ij}, \quad i = 1, 2, 3 \dots N_B \quad (32)$$

where,

$$C_{ij} = \int_{S_B} \frac{\partial}{\partial \hat{n}_j} \left(\frac{1}{r_{ij}} \right) dS + \int_{S_{SW}} \frac{\partial}{\partial \hat{n}_j} \left(\frac{1}{r_{ij}} \right) dS \quad (33)$$

$$= \int_{S_B} \frac{\vec{r}_{ij} \cdot \hat{n}_j}{r_{ij}^3} dS_j + \int_{S_{SW}} \frac{\vec{r}_{ij} \cdot \hat{n}_j}{r_{ij}^3} dS_j$$

$$B_{ij} = \int_{S_B} \frac{1}{r_{ij}} dS_j \quad (34)$$

Herein, C_{ij} and B_{ij} are the influence coefficients on the element j acting on the control point of the element i . N_B is the number of elements on the body surface. After substituting the boundary Eq. (11), the matrix form of Eq. (32) is expressed as:

$$[2\pi\delta - C]_{N_B \times N_B} \{\phi\}_{N_B \times 1}^k = [B]_{N_B \times N_B} \left\{ \frac{\partial\phi}{\partial n} \right\}_{N_B \times 1}^k \quad (35)$$

where, δ_{ij} is the Kronecker delta function. Obviously, to obtain the unit flow potential in each of the six flow conditions, the solution procedure has to be repeated for all the six boundary conditions, being:

$$\left\{ \frac{\partial\phi}{\partial n} \right\}^k = \begin{cases} \alpha & k = 1 \\ \beta & k = 2 \\ \gamma & k = 3 \\ (\gamma y - \beta z) & k = 4 \\ (\alpha z - \gamma x) & k = 5 \\ (\beta x - \alpha y) & k = 6 \end{cases} \quad (36)$$

The computation of the added masses matrix can be performed when the potential $\{\phi\}^k$ has been found for every boundary condition k , and for every element. Equation (28) leads to the following AM matrix:

$$-M_a = -\rho \begin{bmatrix} \sum_{i=1}^{N_B} \phi_i^1 \left\{ \frac{\partial\phi}{\partial n} \right\}_i^1 dS_i & \dots & \sum_{i=1}^{N_B} \phi_i^1 \left\{ \frac{\partial\phi}{\partial n} \right\}_i^6 dS_i \\ \dots & \dots & \dots \\ \sum_{i=1}^{N_B} \phi_i^6 \left\{ \frac{\partial\phi}{\partial n} \right\}_i^1 dS_i & \dots & \sum_{i=1}^{N_B} \phi_i^6 \left\{ \frac{\partial\phi}{\partial n} \right\}_i^6 dS_i \end{bmatrix} \quad (37)$$

The apices in Eq. (37) refer to the condition k , as reported in Eq. (36).

3. Method validation

3.1 Method validation and influence of the mesh definition

This section describes some validation tests carried out to verify the methodology herein described and implemented. The added spheroid (Table 1) masses coefficients of a sphere and of an elongated spheroid have been computed, and the results obtained have been checked against results from the literature, specifically from Refs. [24] and [10]. Following these studies, it is possible to compute analytically the added masses of an ellipsoid having two equal semi-axes ($b=c$):

$$\lambda_{11} = \frac{4}{3} \pi \rho abc \frac{A_0}{2-A_0}; \quad \lambda_{22} = \frac{4}{3} \pi \rho abc \frac{B_0}{2-B_0}; \quad \lambda_{33} = \frac{4}{3} \pi \rho abc \frac{C_0}{2-C_0} \quad (38)$$

are for translational added masses, while the rotational coefficients can be computed as:

$$\begin{aligned} \lambda_{44} &= \frac{4}{15} \frac{\pi \rho abc (b^2 - c^2)^2 (C_0 - B_0)}{2(b^2 - c^2) + (B_0 - C_0)(b^2 + c^2)} \\ \lambda_{55} &= \frac{4}{15} \frac{\pi \rho abc (c^2 - a^2)^2 (A_0 - C_0)}{2(c^2 - a^2) + (C_0 - A_0)(c^2 + a^2)} \\ \lambda_{66} &= \frac{4}{15} \frac{\pi \rho abc (a^2 - b^2)^2 (B_0 - A_0)}{2(a^2 - b^2) + (A_0 - B_0)(a^2 + b^2)} \end{aligned} \quad (39)$$

where, ρ is the density of fluid surrounding the body, a , b , and c are the semi-axes of the ellipsoid, and A_0 , B_0 , and C_0 are coefficients appearing in Eq. (40), which depend only on the shape of the ellipsoid.

$$\begin{aligned} A_0 &= abc \int_0^\infty \frac{du}{(a^2+u)\sqrt{(a^2+u)(b^2+u)(c^2+u)}} \\ B_0 &= abc \int_0^\infty \frac{du}{(b^2+u)\sqrt{(a^2+u)(b^2+u)(c^2+u)}} \\ C_0 &= abc \int_0^\infty \frac{du}{(c^2+u)\sqrt{(a^2+u)(b^2+u)(c^2+u)}} \end{aligned} \quad (40)$$

The analytical computation of all the λ coefficients for a sphere has been carried out by Ref. [10]. According to Lamb's work, which is a reference for airship of traditional configuration, an elongated spheroid of axes a , a , c , having $a < c$ and moving in c direction, presents the coefficient of inertia:

$$\lambda_{11} = \frac{\vartheta}{\vartheta - 1} \quad (41)$$

where,

$$\gamma = \frac{2(1-e^2)}{e^3} \left\{ \frac{1}{2} \log \frac{1+e}{1-e} - e \right\} \quad (42)$$

and where, e is the eccentricity of the longitudinal section:

$$e = \sqrt{1 - \frac{a^2}{c^2}} \quad (43)$$

For the elongated spheroid moving along a direction, the

coefficient:

$$\lambda_{22} = \lambda_{33} = \frac{\delta}{\delta-1} \tag{44}$$

where,

$$\delta = \frac{1}{e^2} - \frac{1-e^2}{2e^3} \log \frac{1+e}{1-e} \tag{45}$$

The rotational added mass of inertia of a spheroid rotating about one of the minor axes is:

$$\lambda_{55} = \lambda_{66} = \frac{e^4(\delta-\vartheta)}{(2-e^2)\{2e^2-(2-e^2)(\delta-\vartheta)\}} \tag{46}$$

where, δ, ϑ, e have the same meaning as reported before. Obviously, λ_{44} is negligible, since the ellipsoid, rotating about the axis coincident to the c axis, doesn't displace fluid.

Table 1. Models used for the validation of the method.

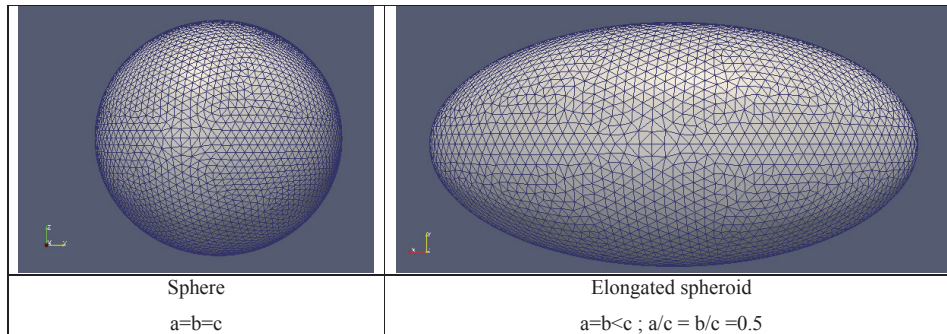


Table 2. Results obtained with the sphere model: trend of added masses matrix coefficients with mesh number of elements.

Lamb's coefficient	0.5	0.5	0.5	0	0	0
Number of elements	A11	A22	A33	A44	A55	A66
1992	0.474	0.474	0.474	-1.39E-06	-1.2E-06	-1,2E-06
3092	0.479	0.479	0.478	-5.47E-07	-6.4E-07	-5.5E-07
4014	0.481	0.481	0.481	-3.68E-07	-3E-07	-3.2E-07
5298	0.484	0.484	0.484	-1.91E-07	-2.1E-07	-2.1E-07
6586	0.485	0.485	0.485	-1.21E-07	-1.3E-07	-1.3E-07
7290	0.486	0.486	0.486	-1.01E-07	-1E-07	-1E-07
8422	0.487	0.487	0.487	-6.98E-08	-8.1E-08	-6.9E-08
9586	0.488	0.488	0.488	-8.03E-08	-6.5E-08	-6.6E-08
10520	0.488	0.488	0.488	-5.56E-08	-4.9E-08	-5.2E-08

Table 3. Error between the expected sphere AM coefficients, and the AM coefficients computed using the proposed approach

Error % (sphere)						
Number of elements	A11	A22	A33	A44	A55	A66
1992	5.247	5.267	5.262	0.000278	0.000231	0.000231
3092	4.226	4.246	4.247	0.000109	0.000128	0.00011
4014	3.723	3.746	3.743	7.36E-05	6.03E-05	6.35E-05
5298	3.251	3.237	3.277	3.82E-05	4.13E-05	4.13E-05
6586	2.923	2.917	2.938	2.42E-05	2.59E-05	2.54E-05
7290	2.776	2.781	2.794	2.01E-05	1.99E-05	2.06E-05
8422	2.586	2.610	2.585	1.4E-05	1.63E-05	1.38E-05
9586	2.404	2.440	2.436	1.61E-05	1.31E-05	1.33E-05
10520	2.300	2.324	2.330	1.11E-05	9.79E-06	1.05E-05

Table 4. Results obtained with the prolate spheroid model: trend of the added masses matrix coefficients with the mesh number of elements.

Lamb's coefficient	0.21	0.704	0.704	0	0.239	0.239
Number of elements	A11	A22	A33	A44	A55	A66
1888	0.2011	0.658	0.659	-1.27E-06	0.214	0.214
3248	0.2032	0.669	0.669	-5.48E-07	0.220	0.220
4256	0.2041	0.674	0.673	-4.19E-07	0.223	0.223
5168	0.2045	0.676	0.677	-2.51E-07	0.224	0.224
6586	0.2053	0.679	0.680	-2.1E-07	0.226	0.226
7290	0.2054	0.680	0.681	-1.96E-07	0.227	0.227
8422	0.2058	0.683	0.682	-1.56E-07	0.228	0.228
9586	0.2061	0.684	0.684	-1.14E-07	0.229	0.229
10520	0.2062	0.685	0.685	-9.64E-08	0.229	0.229

Table 5. Error between the expected elongated spheroid AM coefficients, and the AM coefficients computed using the proposed approach

Error % (Elongated spheroid)						
Number of elements	A11	A22	A33	A44	A55	A66
1888	4.2	6.5	6.4	0.00013	10.5	10.7
3248	3.2	5.0	5.0	5.48E-05	8.1	8.1
4256	2.8	4.4	4.4	4.19E-05	6.9	6.9
5168	2.6	3.9	3.9	2.51E-05	6.4	6.4
6586	2.2	3.5	3.5	2.1E-05	5.4	5.5
7290	2.2	3.4	3.4	1.96E-05	5.2	5.3
8422	2.0	3.1	3.1	1.56E-05	4.8	4.8
9586	1.9	2.8	2.9	1.14E-05	4.6	4.5
10520	1.8	2.8	2.8	9.64E-06	4.4	4.4

As a result, in this case, the surrounding fluid doesn't add any inertia to the angular acceleration of the body.

The λ_{ii} coefficients currently described are dimensional. Their non-dimensional counterparts for the translational AM, following Lamb's approach, are:

$$A_{ii} = \frac{\lambda_{ij}}{4/3\pi\rho abc} \quad (47)$$

where $ii= 11, 22, 33$. It is worth noting that the added masses in the particular cases described (sphere and elongated spheroid) have been converted to a dimensionless form, by dividing the dimensional coefficients by the mass of fluid displaced. The dimensionless form for the rotational AM terms [9] are:

$$A_{44} = \frac{\lambda_{44}}{4/15\pi\rho abc(b^2+c^2)} \quad (48)$$

$$A_{55} = \frac{\lambda_{55}}{4/15\pi\rho abc(a^2+b^2)} \quad (49)$$

$$A_{66} = \frac{\lambda_{66}}{4/15\pi\rho abc(a^2+b^2)} \quad (50)$$

Analytical AM terms obtained by means of Eqs. (37) and (38) are then compared with the data obtained by the Boundary Element Method (BEM). The shapes chosen are a sphere, and a prolate spheroid. To evaluate the dependency of the results from the mesh size, the cases have been investigated for both sphere and ellipsoid. Table 1 reports the geometrical data related to the two meshed shapes used to verify the computational code. These two models have been meshed with an increasing number of elements, in order to show the convergence of the translational and rotational AM coefficients. Tables 2 and 4 show all the dimensionless coefficients for every model, for an increasing number of elements. The exact value, computed with Lamb's formula, is reported at the top of each column. In order to allow the reader to have an idea of the error, Tables 3 and 5 report the percent error between the computed value and Lamb's

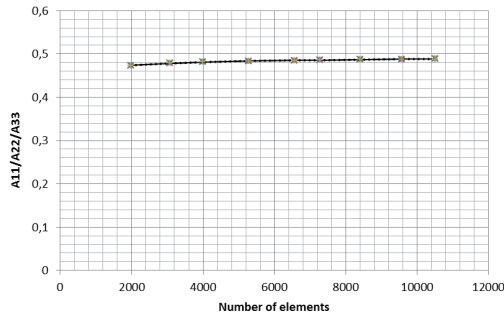


Fig. 4. AM translational coefficients (sphere)

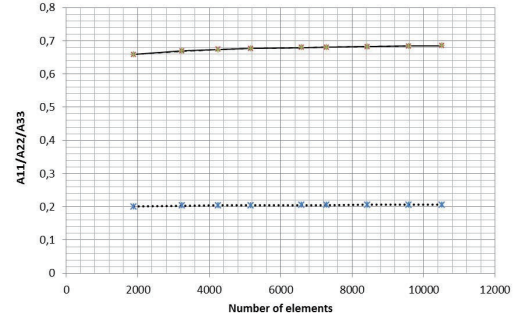


Fig. 6. AM translational coefficients (ellipsoid)

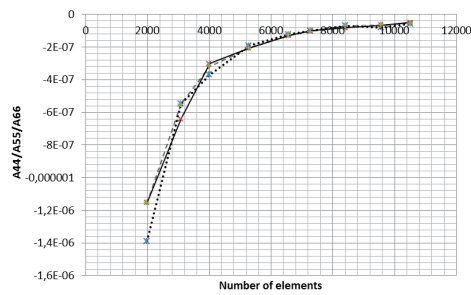


Fig. 5. AM rotational coefficients (sphere)

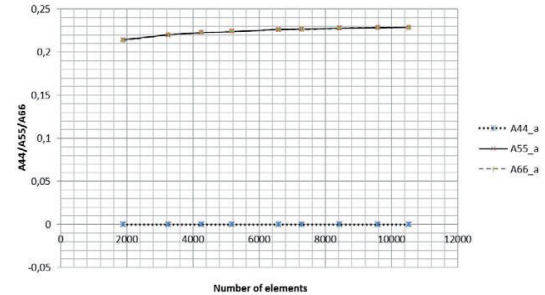


Fig. 7. AM rotational coefficients (ellipsoid)

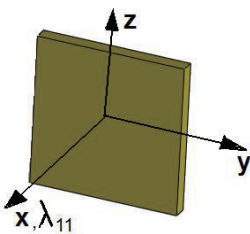
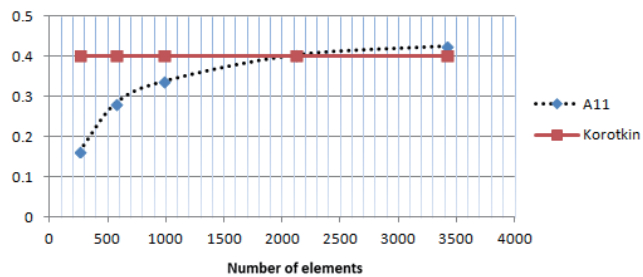


Fig. 8. AM Translational coefficient (plate)



value.

Figures 4 and 6 and Tables 3 and 5 show that an increasing number of elements leads to a reduction of the error on the translational AM coefficients. Figs. 5 and 7 show the same trend, and all the rotational coefficients approach zero, and could be considered negligible, even for a small number of elements. The precision of the method has been also assessed in the computation of the λ_{11} coefficient (along the x axis) for a plate 1m x 1m, with a thickness of 0.1 m. The value computed by the formula included in Ref. [9: 114] is 0.402, as the following Fig. 8 shows, together with the results found for different mesh sizes of the plate.

3.2 Mesh features

The mesh of the body whose added masses are computed requires particular attention. In particular, if symmetries in the body are present, it is important that the mesh respect this symmetry; a loss in mesh symmetry can lead to errors, which can be quite large for the off-diagonal matrix elements.

A strategy to obtain good results is to divide the CAD model along its symmetry axis (one to three); in the following, this half (or 1/4 or 1/8) of the model is meshed, and a mirror operation allows the whole model discretization to be obtained. The meshing operation (Fig. 9) is performed

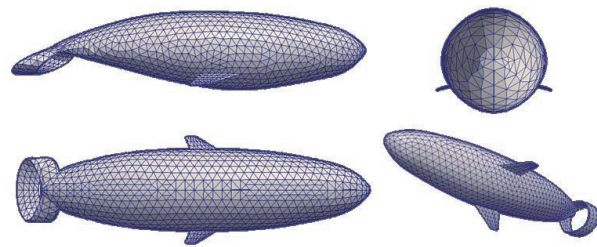


Fig. 9. Symmetric mesh of a body with one plane of symmetry

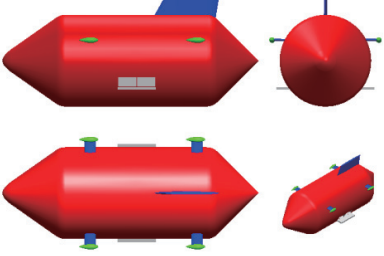
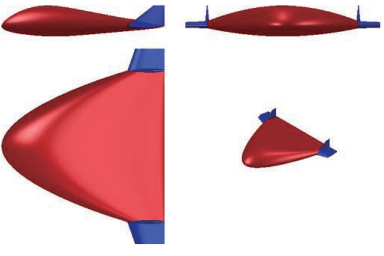
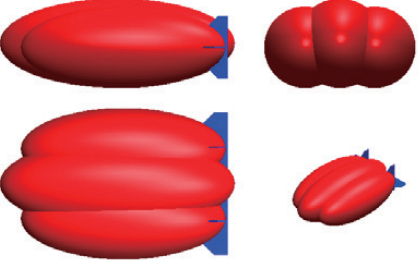
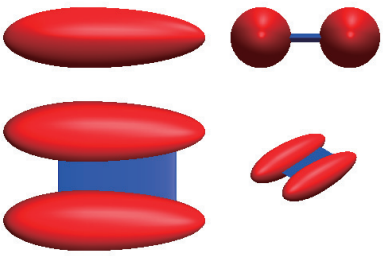
using the approach described for example in Refs. [25, 26], exploiting an algorithm based on the Delaunay triangulation [27]. Tables 2-5 address the influence of the mesh density on the added masses coefficients.

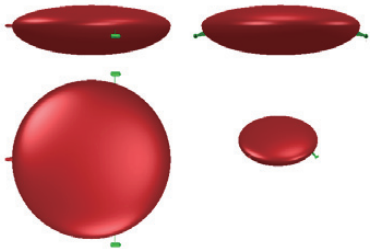
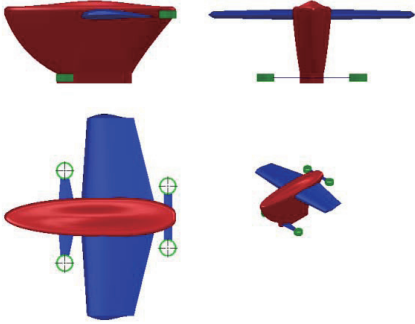
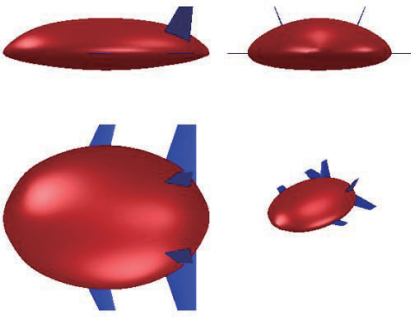
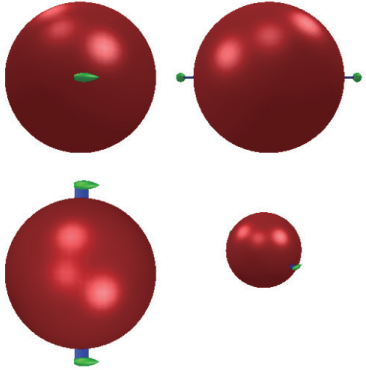
4. Added masses for airships and balloons

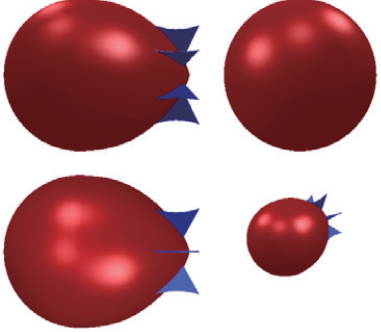
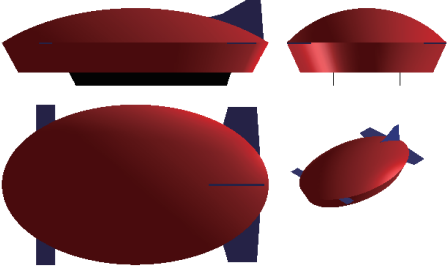
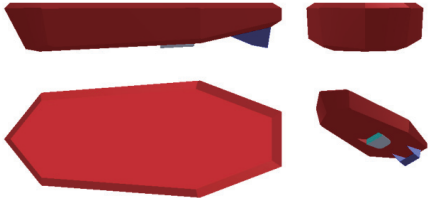
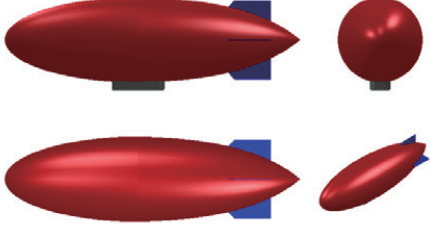
Although new airship configurations have been introduced by several researchers, engineers, and industrial designers, the computation of added masses for these configurations is still a painstaking operation, since the only data available are from Lamb [10], which can only be applied to elliptical bodies. The accurate evaluation of AM for balloons and

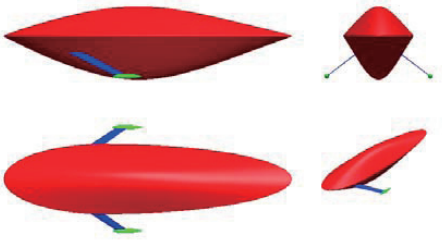
Table 6. AM for some unconventional airship configurations

	Picture of the airship configuration	Added masses matrix coefficients					
		$\begin{bmatrix} X_u & X_v & X_w & X_p & X_q & X_r \\ Y_u & Y_v & Y_w & Y_p & Y_q & Y_r \\ Z_u & Z_v & Z_w & Z_p & Z_q & Z_r \\ K_u & K_v & K_w & K_p & K_q & K_r \\ M_u & M_v & M_w & M_p & M_q & M_r \\ N_u & N_v & N_w & N_p & N_q & N_r \end{bmatrix}$					
1	<p>Configuration inspired by the designer Reindy Allendra http://allendra.carbonmade.com/</p>	2.2E-3	0	-1.05E-3	0	5.59E-5	0
			2.14E-2	0	1.21E-4	0	-3.05E-4
				2.64E-2	0	-8.18E-4	0
					1.46E-5	0	-2.28E-5
			symm			9.87E-4	0
							6.86E-4
2	<p>Configuration inspired by the "Manned Cloud" concept by Jean-Marie Massaud http://www.massaud.com/site/en/#/works/design/transport</p>	1.56E-3	0	-5.42E-4	0	5.964E-5	0
			1.5E-2	0	-2.33E-4	0	-2.76E-4
				1.83E-2	0	-4.097E-4	0
					2.29E-6	0	-8.66E-6
			Symm			5.463E-4	0
							3.67E-4

<p>3</p>	 <p>Configuration inspired by the “The flying yacht” concept (http://www.theflyingyacht.com/)</p>	<table border="1"> <tbody> <tr> <td>1.25E-2</td> <td>0</td> <td>7.21E-5</td> <td>0</td> <td>2.222E-4</td> <td>0</td> </tr> <tr> <td></td> <td>5.54E-2</td> <td>0</td> <td>-1.050E-3</td> <td>0</td> <td>1.842E-2</td> </tr> <tr> <td></td> <td></td> <td>5.3E-2</td> <td>0</td> <td>-1.726E-2</td> <td>0</td> </tr> <tr> <td></td> <td></td> <td></td> <td>4.888E-5</td> <td>0</td> <td>-3.189E-04</td> </tr> <tr> <td></td> <td>Symm</td> <td></td> <td></td> <td>6.936E-3</td> <td>0</td> </tr> <tr> <td></td> <td></td> <td></td> <td></td> <td></td> <td>7.467E-03</td> </tr> </tbody> </table>	1.25E-2	0	7.21E-5	0	2.222E-4	0		5.54E-2	0	-1.050E-3	0	1.842E-2			5.3E-2	0	-1.726E-2	0				4.888E-5	0	-3.189E-04		Symm			6.936E-3	0						7.467E-03
1.25E-2	0	7.21E-5	0	2.222E-4	0																																	
	5.54E-2	0	-1.050E-3	0	1.842E-2																																	
		5.3E-2	0	-1.726E-2	0																																	
			4.888E-5	0	-3.189E-04																																	
	Symm			6.936E-3	0																																	
					7.467E-03																																	
<p>4</p>	 <p>Configuration inspired by the “Dynairship” concept from the Aereon Company (http://www.aereon.com/pages/DYNAIRSHIPII.html)</p>	<table border="1"> <tbody> <tr> <td>7.884E-3</td> <td>0</td> <td>4.619E-03</td> <td>0</td> <td>8.937E-4</td> <td>0</td> </tr> <tr> <td></td> <td>1.165E-2</td> <td>0</td> <td>-1.166E-5</td> <td>0</td> <td>-2.902E-4</td> </tr> <tr> <td></td> <td></td> <td>1.818E-1</td> <td>0</td> <td>1.309E-2</td> <td>0</td> </tr> <tr> <td></td> <td></td> <td></td> <td>5.428E-3</td> <td>0</td> <td>-1.815E-4</td> </tr> <tr> <td></td> <td>symm</td> <td></td> <td></td> <td>6.451E-3</td> <td>0</td> </tr> <tr> <td></td> <td></td> <td></td> <td></td> <td></td> <td>5.653E-4</td> </tr> </tbody> </table>	7.884E-3	0	4.619E-03	0	8.937E-4	0		1.165E-2	0	-1.166E-5	0	-2.902E-4			1.818E-1	0	1.309E-2	0				5.428E-3	0	-1.815E-4		symm			6.451E-3	0						5.653E-4
7.884E-3	0	4.619E-03	0	8.937E-4	0																																	
	1.165E-2	0	-1.166E-5	0	-2.902E-4																																	
		1.818E-1	0	1.309E-2	0																																	
			5.428E-3	0	-1.815E-4																																	
	symm			6.451E-3	0																																	
					5.653E-4																																	
<p>5</p>	 <p>Configuration inspired by the P.791 concept by Lockheed Martin Company (see http://www.lockheedmartin.com/us/products/p-791.html for further details)</p>	<table border="1"> <tbody> <tr> <td>2.792E-2</td> <td>0</td> <td>-9.789E-5</td> <td>0</td> <td>2,775E-4</td> <td>0</td> </tr> <tr> <td></td> <td>5.432E-2</td> <td>0</td> <td>5,099E-4</td> <td>0</td> <td>-1.836E-4</td> </tr> <tr> <td></td> <td></td> <td>1.490E-1</td> <td></td> <td>-3.282E-4</td> <td>0</td> </tr> <tr> <td></td> <td></td> <td></td> <td>1.016E-3</td> <td></td> <td>1.136E-5</td> </tr> <tr> <td></td> <td>symm</td> <td></td> <td></td> <td>3.739E-3</td> <td>0</td> </tr> <tr> <td></td> <td></td> <td></td> <td></td> <td></td> <td>7.117E-4</td> </tr> </tbody> </table>	2.792E-2	0	-9.789E-5	0	2,775E-4	0		5.432E-2	0	5,099E-4	0	-1.836E-4			1.490E-1		-3.282E-4	0				1.016E-3		1.136E-5		symm			3.739E-3	0						7.117E-4
2.792E-2	0	-9.789E-5	0	2,775E-4	0																																	
	5.432E-2	0	5,099E-4	0	-1.836E-4																																	
		1.490E-1		-3.282E-4	0																																	
			1.016E-3		1.136E-5																																	
	symm			3.739E-3	0																																	
					7.117E-4																																	
<p>6</p>	 <p>Configuration inspired by the Nautilus/Polytechnic of Turin Double-hull airship designed by M. Battipede, M. Lando, P.A. Gili, P. Vercesi (www.citation.com)</p>	<table border="1"> <tbody> <tr> <td>1.218E-2</td> <td>0</td> <td>0</td> <td>0</td> <td>0</td> <td>0</td> </tr> <tr> <td></td> <td>5.304E-2</td> <td>0</td> <td>0</td> <td>0</td> <td>-1.166E-4</td> </tr> <tr> <td></td> <td></td> <td>1.348E-1</td> <td>0</td> <td>-4.12E-3</td> <td>0</td> </tr> <tr> <td></td> <td></td> <td></td> <td>2.997E-3</td> <td>0</td> <td>0</td> </tr> <tr> <td></td> <td>symm</td> <td></td> <td></td> <td>3.06E-3</td> <td>0</td> </tr> <tr> <td></td> <td></td> <td></td> <td></td> <td></td> <td>2.021E-3</td> </tr> </tbody> </table>	1.218E-2	0	0	0	0	0		5.304E-2	0	0	0	-1.166E-4			1.348E-1	0	-4.12E-3	0				2.997E-3	0	0		symm			3.06E-3	0						2.021E-3
1.218E-2	0	0	0	0	0																																	
	5.304E-2	0	0	0	-1.166E-4																																	
		1.348E-1	0	-4.12E-3	0																																	
			2.997E-3	0	0																																	
	symm			3.06E-3	0																																	
					2.021E-3																																	

7	 <p>Configuration inspired by the “Alize disc” from P. Balaskovic, LTA corporation (www.operation-lta.com).</p>	<table border="1"> <tbody> <tr><td>2.933E-2</td><td>0</td><td>-9.298E-5</td><td>0</td><td>-9.63E-4</td><td>0</td></tr> <tr><td></td><td>2.927E-2</td><td>0</td><td>1.017E-3</td><td>0</td><td>3.704E-6</td></tr> <tr><td></td><td></td><td>2.345E-1</td><td>0</td><td>2,576E-4</td><td>0</td></tr> <tr><td></td><td></td><td></td><td>5.485E-3</td><td>0</td><td>5.854E-7</td></tr> <tr><td></td><td>symm</td><td></td><td></td><td>5.495E-3</td><td>0</td></tr> <tr><td></td><td></td><td></td><td></td><td></td><td>1.671E-5</td></tr> </tbody> </table>	2.933E-2	0	-9.298E-5	0	-9.63E-4	0		2.927E-2	0	1.017E-3	0	3.704E-6			2.345E-1	0	2,576E-4	0				5.485E-3	0	5.854E-7		symm			5.495E-3	0						1.671E-5
2.933E-2	0	-9.298E-5	0	-9.63E-4	0																																	
	2.927E-2	0	1.017E-3	0	3.704E-6																																	
		2.345E-1	0	2,576E-4	0																																	
			5.485E-3	0	5.854E-7																																	
	symm			5.495E-3	0																																	
					1.671E-5																																	
8	 <p>Configuration inspired by the “Airship One” designed by Gosha Galitsky (http://www.coroflot.com/gosha_id/AirShipOne/1)</p>	<table border="1"> <tbody> <tr><td>9.375E-3</td><td>0</td><td>-6.291E-4</td><td>0</td><td>5.136E-4</td><td>0</td></tr> <tr><td></td><td>7.832E-2</td><td>0</td><td>-8.446E-5</td><td>0</td><td>-2.649E-3</td></tr> <tr><td></td><td></td><td>8.641E-2</td><td>0</td><td>-5.676E-3</td><td>0</td></tr> <tr><td></td><td></td><td></td><td>4.407E-3</td><td></td><td>-1.132E-4</td></tr> <tr><td></td><td>symm</td><td></td><td></td><td>1.548E-3</td><td>0</td></tr> <tr><td></td><td></td><td></td><td></td><td></td><td>1.960E-3</td></tr> </tbody> </table>	9.375E-3	0	-6.291E-4	0	5.136E-4	0		7.832E-2	0	-8.446E-5	0	-2.649E-3			8.641E-2	0	-5.676E-3	0				4.407E-3		-1.132E-4		symm			1.548E-3	0						1.960E-3
9.375E-3	0	-6.291E-4	0	5.136E-4	0																																	
	7.832E-2	0	-8.446E-5	0	-2.649E-3																																	
		8.641E-2	0	-5.676E-3	0																																	
			4.407E-3		-1.132E-4																																	
	symm			1.548E-3	0																																	
					1.960E-3																																	
9	 <p>Configuration inspired by the ML866 airship designed by Aeroscraft (www.aerosml.com)</p>	<table border="1"> <tbody> <tr><td>1.252E-2</td><td>0</td><td>0</td><td>0</td><td>1.263E-3</td><td></td></tr> <tr><td></td><td>2.404E-2</td><td>0</td><td>-1.293E-3</td><td>0</td><td>0</td></tr> <tr><td></td><td></td><td>1.613E-1</td><td>0</td><td>0</td><td>0</td></tr> <tr><td></td><td></td><td></td><td>1.937E-3</td><td>0</td><td>0</td></tr> <tr><td></td><td>symm</td><td></td><td></td><td>4.957E-3</td><td>0</td></tr> <tr><td></td><td></td><td></td><td></td><td></td><td>2.501E-4</td></tr> </tbody> </table>	1.252E-2	0	0	0	1.263E-3			2.404E-2	0	-1.293E-3	0	0			1.613E-1	0	0	0				1.937E-3	0	0		symm			4.957E-3	0						2.501E-4
1.252E-2	0	0	0	1.263E-3																																		
	2.404E-2	0	-1.293E-3	0	0																																	
		1.613E-1	0	0	0																																	
			1.937E-3	0	0																																	
	symm			4.957E-3	0																																	
					2.501E-4																																	
10	 <p>Configuration inspired by the concept by Personal Blimp Company (www.personalblimp.com)</p>	<table border="1"> <tbody> <tr><td>2.553E-1</td><td>0</td><td>0</td><td>0</td><td>0</td><td>0</td></tr> <tr><td></td><td>2.542E-1</td><td>0</td><td>0</td><td>0</td><td>2.85E-3</td></tr> <tr><td></td><td></td><td>2.565E-1</td><td>0</td><td>-2.859E-3</td><td>0</td></tr> <tr><td></td><td></td><td></td><td>1.844E-4</td><td>0</td><td>0</td></tr> <tr><td></td><td>symm</td><td></td><td></td><td>3.243E-5</td><td>0</td></tr> <tr><td></td><td></td><td></td><td></td><td></td><td>6.286E-5</td></tr> </tbody> </table>	2.553E-1	0	0	0	0	0		2.542E-1	0	0	0	2.85E-3			2.565E-1	0	-2.859E-3	0				1.844E-4	0	0		symm			3.243E-5	0						6.286E-5
2.553E-1	0	0	0	0	0																																	
	2.542E-1	0	0	0	2.85E-3																																	
		2.565E-1	0	-2.859E-3	0																																	
			1.844E-4	0	0																																	
	symm			3.243E-5	0																																	
					6.286E-5																																	

11	 <p>Configuration inspired by the spherical airship by the 21st Century Airships Inc. (www.21stcenturyairship.com)</p>	<table border="1"> <tbody> <tr><td>2.721E-1</td><td>0</td><td>0</td><td>0</td><td>0</td><td>0</td></tr> <tr><td></td><td>2.719E-1</td><td>0</td><td>0</td><td>0</td><td>-3.555E-3</td></tr> <tr><td></td><td></td><td>2.691E-1</td><td>0</td><td>3.556E-3</td><td>0</td></tr> <tr><td></td><td></td><td></td><td>2.697E-5</td><td>0</td><td>0</td></tr> <tr><td></td><td>symm</td><td></td><td></td><td>5.805E-4</td><td>0</td></tr> <tr><td></td><td></td><td></td><td></td><td></td><td>5.524E-4</td></tr> </tbody> </table>	2.721E-1	0	0	0	0	0		2.719E-1	0	0	0	-3.555E-3			2.691E-1	0	3.556E-3	0				2.697E-5	0	0		symm			5.805E-4	0						5.524E-4
2.721E-1	0	0	0	0	0																																	
	2.719E-1	0	0	0	-3.555E-3																																	
		2.691E-1	0	3.556E-3	0																																	
			2.697E-5	0	0																																	
	symm			5.805E-4	0																																	
					5.524E-4																																	
12	 <p>Configuration inspired by the SkyFreighter concept by Millenium Airship (www.milleniumairship.com)</p>	<table border="1"> <tbody> <tr><td>9.687E-3</td><td>0</td><td>1.365E-4</td><td>0</td><td>-8.811E-4</td><td>0</td></tr> <tr><td></td><td>3.54E-2</td><td>0</td><td>1,274E-3</td><td>0</td><td>5,752E-4</td></tr> <tr><td></td><td></td><td>9.976E-2</td><td>0</td><td>-4.363E-4</td><td>0</td></tr> <tr><td></td><td></td><td></td><td>5.801E-4</td><td>0</td><td>5.092E-5</td></tr> <tr><td></td><td>symm</td><td></td><td></td><td>2.501E-3</td><td>0</td></tr> <tr><td></td><td></td><td></td><td></td><td></td><td>4.393E-4</td></tr> </tbody> </table>	9.687E-3	0	1.365E-4	0	-8.811E-4	0		3.54E-2	0	1,274E-3	0	5,752E-4			9.976E-2	0	-4.363E-4	0				5.801E-4	0	5.092E-5		symm			2.501E-3	0						4.393E-4
9.687E-3	0	1.365E-4	0	-8.811E-4	0																																	
	3.54E-2	0	1,274E-3	0	5,752E-4																																	
		9.976E-2	0	-4.363E-4	0																																	
			5.801E-4	0	5.092E-5																																	
	symm			2.501E-3	0																																	
					4.393E-4																																	
13	 <p>Configuration inspired by Strato Cruiser Concept by T. Schaedler and M.J. Brown (http://www.dezeen.com/2007/10/08/strato-cruiser-airship-concept-by-tino-schaedler-and-michael-j-brown/)</p>	<table border="1"> <tbody> <tr><td>4.756E-3</td><td>0</td><td>-1.46E-3</td><td>0</td><td>-5.997E-4</td><td>0</td></tr> <tr><td></td><td>1.585E-2</td><td>0</td><td>8.351E-5</td><td>0</td><td>4.662E-4</td></tr> <tr><td></td><td></td><td>6.964E-2</td><td>0</td><td>1.823E-3</td><td>0</td></tr> <tr><td></td><td></td><td></td><td>2.061E-4</td><td>0</td><td>-6.245E-6</td></tr> <tr><td></td><td>Symm</td><td></td><td></td><td>2.538E-3</td><td>0</td></tr> <tr><td></td><td></td><td></td><td></td><td></td><td>4.218E-4</td></tr> </tbody> </table>	4.756E-3	0	-1.46E-3	0	-5.997E-4	0		1.585E-2	0	8.351E-5	0	4.662E-4			6.964E-2	0	1.823E-3	0				2.061E-4	0	-6.245E-6		Symm			2.538E-3	0						4.218E-4
4.756E-3	0	-1.46E-3	0	-5.997E-4	0																																	
	1.585E-2	0	8.351E-5	0	4.662E-4																																	
		6.964E-2	0	1.823E-3	0																																	
			2.061E-4	0	-6.245E-6																																	
	Symm			2.538E-3	0																																	
					4.218E-4																																	
14	 <p>Traditional Configuration inspired by the Skyship 600 airship by Airship Industries (http://en.wikipedia.org/wiki/Airship_Industries_Skyship_600)</p>	<table border="1"> <tbody> <tr><td>4.27E-3</td><td>0</td><td>-3.535E-6</td><td>0</td><td>1.230E-5</td><td>0</td></tr> <tr><td></td><td>3.353E-2</td><td>0</td><td>-5.594E-5</td><td>0</td><td>-1.261E-4</td></tr> <tr><td></td><td></td><td>3.194E-02</td><td>0</td><td>9,841E-5</td><td>0</td></tr> <tr><td></td><td></td><td></td><td>4,977E-6</td><td></td><td>1.827E-6</td></tr> <tr><td></td><td>symm</td><td></td><td></td><td>1.002E-3</td><td>0</td></tr> <tr><td></td><td></td><td></td><td></td><td></td><td>1.029E-3</td></tr> </tbody> </table>	4.27E-3	0	-3.535E-6	0	1.230E-5	0		3.353E-2	0	-5.594E-5	0	-1.261E-4			3.194E-02	0	9,841E-5	0				4,977E-6		1.827E-6		symm			1.002E-3	0						1.029E-3
4.27E-3	0	-3.535E-6	0	1.230E-5	0																																	
	3.353E-2	0	-5.594E-5	0	-1.261E-4																																	
		3.194E-02	0	9,841E-5	0																																	
			4,977E-6		1.827E-6																																	
	symm			1.002E-3	0																																	
					1.029E-3																																	

<p>15</p>  <p>Configuration inspired by the “Stalker Airship” by K. Judlin for Yanko Design http://www.yankodesign.com/2008/07/14/stalker-symbiotic-exploration-in-the-year-xxii/</p>	<table border="1"> <tr><td>6.816E-4</td><td>0</td><td>-9.987E-6</td><td>0</td><td>7.625E-4</td><td>0</td></tr> <tr><td></td><td>6.033E-3</td><td>0</td><td>-4.739E-6</td><td>0</td><td>3.525E-5</td></tr> <tr><td></td><td></td><td>9.740E-2</td><td>0</td><td>-2.263E-4</td><td>0</td></tr> <tr><td></td><td></td><td></td><td>1.477E-5</td><td>0</td><td>-9.776E-8</td></tr> <tr><td></td><td>symm</td><td></td><td></td><td>2.514E-3</td><td>0</td></tr> <tr><td></td><td></td><td></td><td></td><td></td><td>1.453E-4</td></tr> </table>	6.816E-4	0	-9.987E-6	0	7.625E-4	0		6.033E-3	0	-4.739E-6	0	3.525E-5			9.740E-2	0	-2.263E-4	0				1.477E-5	0	-9.776E-8		symm			2.514E-3	0						1.453E-4
6.816E-4	0	-9.987E-6	0	7.625E-4	0																																
	6.033E-3	0	-4.739E-6	0	3.525E-5																																
		9.740E-2	0	-2.263E-4	0																																
			1.477E-5	0	-9.776E-8																																
	symm			2.514E-3	0																																
					1.453E-4																																
<p>16</p>  <p>Configuration inspired by the “Skylifter Airship” configuration proposed by the Skylifter Company http://skylifter.com.au/</p>	<table border="1"> <tr><td>1.511E-2</td><td>0</td><td>0</td><td>0</td><td>1.514E-3</td><td>0</td></tr> <tr><td></td><td>1.511E-02</td><td>0</td><td>-1.533E-3</td><td>0</td><td>0</td></tr> <tr><td></td><td></td><td>2.835E-01</td><td>0</td><td>0</td><td>0</td></tr> <tr><td></td><td></td><td></td><td>8.507E-03</td><td>0</td><td>0</td></tr> <tr><td></td><td>symm</td><td></td><td></td><td>8.525E-03</td><td>0</td></tr> <tr><td></td><td></td><td></td><td></td><td></td><td>0</td></tr> </table>	1.511E-2	0	0	0	1.514E-3	0		1.511E-02	0	-1.533E-3	0	0			2.835E-01	0	0	0				8.507E-03	0	0		symm			8.525E-03	0						0
1.511E-2	0	0	0	1.514E-3	0																																
	1.511E-02	0	-1.533E-3	0	0																																
		2.835E-01	0	0	0																																
			8.507E-03	0	0																																
	symm			8.525E-03	0																																
					0																																

unconventional airships cannot be achieved through the conventional formulas used for ellipsoids, even though they could be used as useful comparison data. Tables 6 and 7 present some unconventional configurations of airships and some typical hot air balloons shapes, together with their added masses coefficients. It is worth noting that all the configurations proposed here are inspired by real concepts documented in scientific papers and websites. About the axis reference system, as explained in the first insert, the X axis is longitudinal, and points towards the nose of the configuration, the Y axis lies in the lateral direction, pointing the right side of the body, while the Z axis is vertical, oriented to the top of the shape. The origin of the reference system is centered in the centre of volume of the configurations.

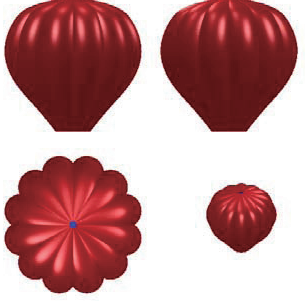
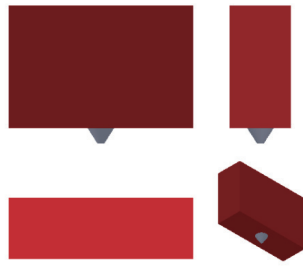
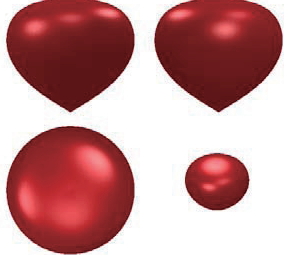
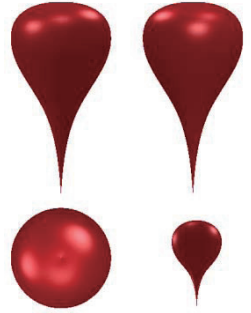
5. Discussions

One of the configurations presented (#3) does not present any plane of symmetry; the off-the-diagonal values are quite high, if compared to the translational and rotational element lying on-the-diagonal, and the matrix is sparse, with a few elements with zero value. Configurations #1, #2, #3, #4, #5, #7, #8, #9, #12, #13, #14, and #15 present a single longitudinal plane of symmetry; in this case, the added masses matrix

shows six (6) off-diagonal elements whose value are different from zero. Configurations #6, #10, #11, #16, #17, #18, #19, and #20 present two planes of symmetry; out-of-diagonal terms in the matrix show low values, and only two off-diagonal cells are different from zero. Their absolute value tends to the same result, if the object has axial symmetry property about an axis.

It is worth noticing that the terms in the matrix are dimensionless; hence, the shapes that are similar to a sphere present values of the translational terms that are more or less half the values reported by Lamb [10]. In Lamb’s work, the dimensionless variables were based on the volume of the sphere, $4/3 \pi r^3$, while here the cube of length $(2r)^3$ is used, hence the ratio is about 2. When the body is axial-symmetric and streamlined, the difference in the diagonal translational terms tend to be larger, with two terms equal in value. On the other hand, complex shapes, like configurations #16, #19, and #20, present null values of rotation element around the Z axis; these bodies are perfectly axial-symmetric, so that a rotation around the Z axis does not displace fluid. The configuration #17 represent a shape similar to an hot air balloon with gores, and in this case a rotation around the Z axis moves a part of fluid, so that the correspondingly value in the added masses matrix is different from zero. Values found for spheres or oblate spheroids presenting

Table 7. AM for balloon configurations

	Picture of balloon configuration	Added masses matrix coefficients																																				
17	 <p>Typical hot air balloon configuration inspired by the Ultramagic manufacturer design (www.ultramagic.com)</p>	<table border="1"> <tr> <td>2.283E-1</td> <td>0</td> <td>0</td> <td>0</td> <td>-6.782E-4</td> <td>0</td> </tr> <tr> <td></td> <td>2.282E-1</td> <td>0</td> <td>6.766E-4</td> <td>0</td> <td>0</td> </tr> <tr> <td></td> <td></td> <td>2.38E-1</td> <td>0</td> <td>0</td> <td>0</td> </tr> <tr> <td></td> <td></td> <td></td> <td>1.248E-3</td> <td>0</td> <td>0</td> </tr> <tr> <td></td> <td>Symm</td> <td></td> <td></td> <td>1.245E-3</td> <td>0</td> </tr> <tr> <td></td> <td></td> <td></td> <td></td> <td></td> <td>1.128E-3</td> </tr> </table>	2.283E-1	0	0	0	-6.782E-4	0		2.282E-1	0	6.766E-4	0	0			2.38E-1	0	0	0				1.248E-3	0	0		Symm			1.245E-3	0						1.128E-3
2.283E-1	0	0	0	-6.782E-4	0																																	
	2.282E-1	0	6.766E-4	0	0																																	
		2.38E-1	0	0	0																																	
			1.248E-3	0	0																																	
	Symm			1.245E-3	0																																	
					1.128E-3																																	
18	 <p>Special shape hot air balloon inspired by the Cameron manufacturer design[6]</p>	<table border="1"> <tr> <td>1.415E-1</td> <td>0</td> <td>0</td> <td>0</td> <td>-2.763E-2</td> <td>0</td> </tr> <tr> <td></td> <td>1.863E-1</td> <td>0</td> <td>-1.197E-4</td> <td>0</td> <td>0</td> </tr> <tr> <td></td> <td></td> <td>6.467E-1</td> <td>0</td> <td>0</td> <td>0</td> </tr> <tr> <td></td> <td></td> <td></td> <td>4.781E-3</td> <td>0</td> <td>0</td> </tr> <tr> <td></td> <td>symm</td> <td></td> <td></td> <td>1.18E-2</td> <td>0</td> </tr> <tr> <td></td> <td></td> <td></td> <td></td> <td></td> <td>1.14E-2</td> </tr> </table>	1.415E-1	0	0	0	-2.763E-2	0		1.863E-1	0	-1.197E-4	0	0			6.467E-1	0	0	0				4.781E-3	0	0		symm			1.18E-2	0						1.14E-2
1.415E-1	0	0	0	-2.763E-2	0																																	
	1.863E-1	0	-1.197E-4	0	0																																	
		6.467E-1	0	0	0																																	
			4.781E-3	0	0																																	
	symm			1.18E-2	0																																	
					1.14E-2																																	
19	 <p>Spherical scientific balloon at medium altitude put reference [6]</p>	<table border="1"> <tr> <td>1.888E-1</td> <td>0</td> <td>0</td> <td>0</td> <td>1.271E-3</td> <td>0</td> </tr> <tr> <td></td> <td>1.888E-1</td> <td>0</td> <td>-1.268E-3</td> <td>0</td> <td>0</td> </tr> <tr> <td></td> <td></td> <td>2.672E-1</td> <td></td> <td>0</td> <td>0</td> </tr> <tr> <td></td> <td></td> <td></td> <td>1.466E-3</td> <td>0</td> <td>0</td> </tr> <tr> <td></td> <td>Symm</td> <td></td> <td></td> <td>1.465E-3</td> <td>0</td> </tr> <tr> <td></td> <td></td> <td></td> <td></td> <td></td> <td>0</td> </tr> </table>	1.888E-1	0	0	0	1.271E-3	0		1.888E-1	0	-1.268E-3	0	0			2.672E-1		0	0				1.466E-3	0	0		Symm			1.465E-3	0						0
1.888E-1	0	0	0	1.271E-3	0																																	
	1.888E-1	0	-1.268E-3	0	0																																	
		2.672E-1		0	0																																	
			1.466E-3	0	0																																	
	Symm			1.465E-3	0																																	
					0																																	
20	 <p>Spherical scientific balloon at low altitude put reference [6]</p>	<table border="1"> <tr> <td>2.984E-1</td> <td>0</td> <td>0</td> <td>0</td> <td>9.279E-3</td> <td>0</td> </tr> <tr> <td></td> <td>2.985E-1</td> <td>0</td> <td>-9.265E-3</td> <td>0</td> <td>0</td> </tr> <tr> <td></td> <td></td> <td>2.367E-1</td> <td>0</td> <td>0</td> <td>0</td> </tr> <tr> <td></td> <td></td> <td></td> <td>9.208E-3</td> <td>0</td> <td>0</td> </tr> <tr> <td></td> <td>symm</td> <td></td> <td></td> <td>9.225E-3</td> <td>0</td> </tr> <tr> <td></td> <td></td> <td></td> <td></td> <td></td> <td>0</td> </tr> </table>	2.984E-1	0	0	0	9.279E-3	0		2.985E-1	0	-9.265E-3	0	0			2.367E-1	0	0	0				9.208E-3	0	0		symm			9.225E-3	0						0
2.984E-1	0	0	0	9.279E-3	0																																	
	2.985E-1	0	-9.265E-3	0	0																																	
		2.367E-1	0	0	0																																	
			9.208E-3	0	0																																	
	symm			9.225E-3	0																																	
					0																																	

three planes of symmetry have already been presented in the section dealing with validation; in this case, the elements in the mass matrixes are all null, except the values A_{11} , A_{22} , A_{33} , A_{44} , and A_{55} , as already found by Lamb. The increase in precision obtainable with the application of the coefficients presented in this paper can be evaluated by comparing the results with the equivalent ellipsoid method, which is currently suggested by the literature [2] for unconventional shapes. Due to the difference between the Lamb and the SNAME [21] methods to obtain dimensionless quantities, some corrections should be applied. Two shapes will be considered: #12, which represents a complex shape; and #14, which is close to an axial-symmetric ellipsoidal shape. First, an equivalent ellipsoid with longitudinal semi-axis a and

lateral and vertical semi-axes equal to b is found for shapes #12 and #14. Considering the same volume (Vol) and length (l) of the real shape, it follows that:

$$b = \sqrt{\frac{3Vol}{4\pi a}} \tag{51}$$

An a/b ratio can be so found for configurations #12 and #14, and values of k_1 , k_2 , and k' can be found from the Table included in the paper by Lamb [10], as Fig.9 shows.

Table 8 summarizes the results obtained, in terms of ellipsoid fitness ratio, and coefficients.

To compare added masses coefficients obtained with the dimensionless one from Ref. [21] adopted here (A_{ij}), the following relations should be considered:

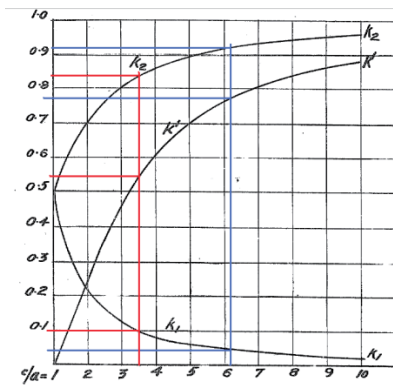


Fig. 10. k_1 , k_2 , k' coefficients from Lamb report [Lamb, H.]

$$\begin{cases} X_{\dot{u}} = A_{11}\rho l^3 = k_1\rho\frac{4}{3}\pi ab^2 \\ Y_{\dot{v}} = A_{22}\rho l^3 = k_2\rho\frac{4}{3}\pi ab^2 \\ Z_{\dot{w}} = A_{33}\rho l^3 = k_2\rho\frac{4}{3}\pi ab^2 \\ K_{\dot{p}} = 0 \\ M_{\dot{q}} = A_{55}\rho l^5 = k'\rho\frac{4}{3}\pi ab^2\frac{(a^2+b^2)}{5} \\ N_{\dot{r}} = A_{66}\rho l^5 = k'\rho\frac{4}{3}\pi ab^2\frac{(a^2+b^2)}{5} \end{cases} \tag{52}$$

With $l=2a$, and calling $\tau=a/b$, this leads to:

$$\begin{aligned} A_{11} &= \frac{\pi}{6\tau^2}k_1; A_{22} = \frac{\pi}{6\tau^2}k_2; A_{33} = \frac{\pi}{6\tau^2}k_2; A_{44} \\ &= 0; A_{55} = \frac{k'\pi(\tau^2+1)}{24 \cdot 5\tau^4}; A_{66} = \frac{k'\pi(\tau^2+1)}{24 \cdot 5\tau^4} \end{aligned} \tag{53}$$

Table 8. Lamb's AM coefficients for Configurations 12 and 14.

	a/b	K_1	K_2	K'
Config#12	6.13	0.045	0.92	0.77
Config #14	3.57	0.1	0.83	0.54

Table 9 shows a comparison between coefficients computed with the proposed method, and by the methodology by Lamb based on the equivalent ellipsoid. The table clearly shows how applying the equivalent ellipsoid

Table 9. AM matrix coefficients for Configurations 12, 14.

Config.		A_{11}	A_{22}	A_{33}	A_{44}	A_{55}	A_{66}
#12	Proposed method on real shape	9.69E-3	9.97E-2	3.54E-2	5.8E-4	4.4E-4	2.5E-3
	Lamb method on equivalent ellipsoid	6.2E-4	1.28E-2	1.28E-2	0	5.51E-4	5.51E-4
	Equiv. ellipsoid vs. Real shape difference	-93.6%	-87.2%	-63.8%	-	+25.2%	-78%
#14	Proposed method on real shape	4.27E-3	3.19E-2	3.35E-2	4.98E-6	1.02E-3	1.03E-3
	Lamb method on equivalent ellipsoid	4.11E-3	3.41E-2	3.41E-2	0	1.19E-3	1.19E-3
	Equiv. ellipsoid vs. Real shape difference	-3.75%	+6.9%	+1.79%	/	+16.7%	+15.5%

method to a traditional airship shape, like config. #14, leads to small errors; on the other hand, applying the equivalent ellipsoid method to an unconventional shape with complex shape (e.g. config. #12) can introduce significant errors. The added masses contribution is critical, when modeling the dynamic of systems like airships, hot air balloons, and submarine vehicles; for instance, by computing the acceleration of a sphere ($\lambda=0.5$), and neglecting the added masses contribution, a 50% error with respect to the correct value is obtained, with a consequent overestimation of the acceleration.

Acknowledgments

This research has been supported by the European Union, Seventh Framework Programme (FP7/2007-2013) under grant agreement n° FP7-AAT GA-2011-285602-MAAT-Multibody Advanced Airship for Transport.

References

- [1] Khoury, G.A., and Gillet, J.D., "Airship Technology", Cambridge University Press, Cambridge, UK, 1999.
- [2] Carichner, G.E., and Nicolai, L., , "Fundamentals of Aircraft and Airship Design, Volume Two - Airship Design and Case Studies", AIAA Education Series, April 2013, ISBN-13: 978-1600868986.
- [3] Ceruti, A. and Marzocca, P. "Conceptual Approach to Unconventional Airship Design and Synthesis", *J. Aerosp. Eng.*, 2013.
DOI: 10.1061/(ASCE)AS.1943-5525.0000344
- [4] Stockbridge C., Ceruti A. and Marzocca P., "Airship Research and Development in the Areas of Design, Structures, Dynamics and Energy Systems", *International Journal Aeronautical and Space Sciences* Vol. 13, No. 2, 2012, pp. 170-187.
- [5] Atkinson, C.J. and Urso, R.G., , "Modelling of Apparent Mass Effect for the Real-Time Simulation of a Hybrid Airship", *AIAA*, New York, 2006, pp. 2006-6619.
- [6] Yajima, N., Izutsu, N., Imamura, T., and Abe, T. "Scientific Ballooning Floating in the Stratosphere and the Atmospheres of Other Planets", *Springer Science, Business Media LLC*, 2009.
DOI: 10.1007/978-0-387-09727-5.
- [7] Hess, J. and Smith, A., "Calculation of Potential Flow about Arbitrary Bodies", *Progress in Aeronautical Sciences*, Vol. 8, 1967.
- [8] Birkhoff, G. "Hydrodynamics". Princeton Univ. Press, Princeton, 1960.
- [9] Korotkin, A.I. "Added mass of ship structure". Fluid mechanics and its applications, Springer, Vol. 88, 2009, ISBN 978-1-4020-9431-6.
- [10] Lamb, H., "The inertia-coefficients of an ellipsoid moving in a fluid", Reports and Memoranda, No. 623, October, 1918.
- [11] Munk, M., "Some Tables of the Factor of Apparent Additional Mass", NACA TN-197, July 1924.
- [12] Implay, F.H., "The Complete Expression for 'Added Mass' of a Rigid Body Moving in an Ideal Fluid", TMB Report 1528, July 1961.
- [13] Lamb G., "Hydrodynamics", Cambridge University Press, Cambridge, 1932.
- [14] Anderson, W.J., Shah, G.N. and Jungsun, P., "Added mass of high-amplitude balloons", *Journal of Aircraft*, Vol. 32, No. 2, 1995, pp. 285-289.
- [15] Lojczanski, L.G., "Mechanics of Fluid and Gas", Nauka, Moscow, 1970.
- [16] Riman, I.S. and Kreps, R.L. "Added masses of bodies of various shape", *Proceedings of Central Institute of Aero- and Hydrodynamics* 635, 1947, pp. 1-46.
- [17] Caspersen, C., Berthelsen, P.A., Eik, M., Pákozdi, C., and Kjendlie, P.L. "Added mass in human swimmers: Age and gender differences", *Journal of Biomechanics*, Vol. 43, No. 12, August 2010, pp. 2369-2373.
- [18] Azouz, N., Chaabani, S., Lerbet, J. and Abichou, A., "Computation of the Added Masses of an Unconventional Airship", *Journal of Applied Mathematics*, Article ID 714627, 19 pages, 2012. DOI:10.1155/2012/714627.
- [19] Bennaceur, S., and Naoufel A., "Contribution of the added masses in the dynamic modelling of flexible airships", *Nonlinear Dynamics*, Vol. 67, No. 1, January 2012, pp. 215-226.
- [20] Brennen, C. E., "A review of added mass and fluid inertial forces", Naval Civil Engineering Laboratory, Port Hueneme, California, January 1982.
- [21] SNAME., "Nomenclature for treating the motion of a submerged body through a fluid", Technical and Research Bulletin 1-5, Hydrodynamics Subcommittee of the Technical and Research Committee, Society of Naval Architects and Marine Engineers, 1950.
- [22] Kats, J. and Plotkin, A., "Low-Speed Aerodynamics 2nd ed.", Cambridge University Press, Cambridge (UK), 2001.
- [23] Becker, A.A., "The Boundary Element Method in Engineering", Mc-Graw Hill, 1992.
- [24] Kochin, N.E., Kibel, I.A., and Rose, N.V., "Theoretical Hydromechanics, Parts I and II" Publisher of Physical and Mathematical Literature, Moscow, 1963.
- [25] Dey, T. K., "Curve and surface reconstruction: algorithms with mathematical analysis", Cambridge University Press, New York, 2006.
- [26] Boissonnat, J.D. and Oudot, S., "Provably good surface sampling and meshing of surfaces", *Graphical Models*, Vol. 67, 2005, pp. 405-451.
- [27] Cheng, S.W., Dey, T. K. and Levine, J., "Theory of a practical Delaunay meshing algorithm for a large class of domains." Algorithms, *Architecture and Information System Security, World Scientific Review*, Vol. 3, 2008, pp. 17-41.